The Sphere Conundrum: Using Voxel-based Dosimetry to evaluate sphere concentration and tumor dose in Hepatocellular Carcinoma treated with Y-90 Radioembolization

Tyler Sandow (tyler.sandow@ochsner.org)
Ochsner Health System https://orcid.org/0000-0002-5788-7357
Juan Gimenez
Ochsner Health System
Kelley Nunez
Ochsner Health System
Richard Tramel
Ochsner Health System
Patrick Gilbert
Ochsner Health System
Brianna Oliver
Ochsner Health System
Michael Cline
Ochsner Health System
Kirk Fowers
Boston Scientific Corp
Ari Cohen
Ochsner Health System
Paul Thevenot
Ochsner Health System

Research Article

Keywords: Radioembolization, Radiation Dosimetry, Sphere concentration, Y90, Image-guided therapy, Hepatocellular carcinoma

Posted Date: May 18th, 2023

DOI: https://doi.org/10.21203/rs.3.rs-2790650/v1

Abstract

Purpose

To evaluate sphere concentration delivered to tumor and non-tumor tissue using voxel-based dosimetry as it relates to treatment, pathologic outcomes, and adverse events.

Methods

A retrospective, single-center analysis of patients (n = 57) with solitary HCC who were treated with Y90 radiation segmentectomy with Y90 glass microsphere infusion (TheraSphere; Boston Scientific, Marlborough, MA, USA) from 2020 to 2022 was performed. Post-treatment dosimetry was evaluated using Mirada DBx Build 1.2.0 Simplicit^{90}Y dosimetry software. Voxel-based dosimetry and MIRD formula were utilized to calculate sphere concentration to tumor and non-tumor tissue. Time to progression (TTP), treatment response, pathologic response, and adverse events were studied.

Results

Fifty-seven patients with solitary tumors were analyzed with a median tumor diameter of 3.4cm (range 1.2-6.8cm). The median tumor absorbed dose was 692Gy (range, 256-1332Gy) with a median perfused treatment volume of 113mL (range, 33.6-442mL). Median sphere activity (SA) at time of delivery was 1428Bq (range, 412-2589Bq). Using voxel-based dosimetry and the MIRD formula, median tumor sphere concentration was 12,339 spheres/mL (range, 2,689 – 37,649 spheres/mL). Sphere concentration to tumor exhibited a weak, inverse correlation with perfused treatment volume (R^2 = 0.25). However, tumor sphere concentration and non-tumor sphere concentration exhibited a direct, positive correlation (R^2 = 0.72). Of the 52 tumors with post-treatment imaging, objective response was noted in 50 patients (96%) and complete response in 41 patients (79%). 98% of all treated tumors demonstrated a durable response at 2 years. The median time to progression for all patients was not reached with a 2-year progression rate of 11%. Multivariate analysis demonstrated target dose as the only statistically significant variable associated with TTP (p = 0.033). 14 patients underwent liver transplant. Median tumor necrosis was 99% (range, 80–100%).

Conclusion

Voxel-based dosimetry following Y90 radioembolization can be utilized to measure sphere concentration into tumor and non-tumoral tissue. Higher SA allows increased tumor absorbed dose with limited sphere/mL tumor capacity.

PURPOSE

The LEGACY study showcased the ablative capabilities of yttrium radioembolization (Y90) for solitary, unresectable hepatocellular carcinoma (HCC) and its effect on overall survival, resulting in the incorporation of radioembolization into the Barcelona Clinic Liver Cancer (BCLC) algorithm for stage 0-A disease [1, 2]. Furthermore, multiple studies have highlighted the effect of generating complete pathologic necrosis (CPN) with unicompartment, perfused radiation doses $\geq$ 190Gy and $\geq$ 400Gy [3-5]. In these studies, higher rates of CPN were achieved with higher radiation doses to the perfused volume [3-5]. Complete/extensive tumor necrosis has also been shown to be strongly associated with lower HCC mortality rates and longer recurrence-free survival [6].

Perfused volume and dose activity play a critical role in delivering ablative doses to tumors [7]. As perfused volume decreases, the absorbed dose to tissue increases for the same delivered activity [7]. Similarly, increasing sphere activity (SA) for the same perfused volume results in greater tissue absorbed dose [7]. However, individual sphere activity (SA) and total sphere count must be appropriately balanced to deliver ablative doses to tumors during radiation segmentectomy [7]. Tokisch et al. demonstrated the importance of microsphere SA in generating CPN, favoring microspheres with *higher* individual SA [5]. Higher SA allows efficient, reproducible delivery of absorbed dose to tumor, which is associated with increased rates of CPN and prolonged time to progression and overall survival [3-5]. On the other hand, increasing the number of microspheres/mL during Y90 delivery leads to increased homogeneity of absorbed dose to *normal* tissue and may result in greater toxicity to a larger fraction of hepatic lobules [8]. A recent study has also shown an increased incidence of adverse events (AEs) in patients who received treatment in larger volumes of nontumoral portions of liver with resin microspheres [9]. Collectively, these findings might suggest that increasing sphere concentration to a larger perfused territory of non-tumoral liver results in higher likelihood of AEs without clinical benefit, as the tumor may become *saturated* and sphere delivery to tumor becomes relatively less efficient.

The purpose of this study is to use Voxel-based dosimetry to explore the relationship of sphere concentration into the tumor bed and radiologic outcomes as well as pathologic outcomes in patients with solitary, unresectable HCC who have received Yttrium-90 (Y90) glass microspheres.

MATERIALS AND METHODS

Study Design and Population

An IRB-approved, single-center, retrospective analysis was performed on patients with solitary, treatment-naive HCC, who were treated with Y90 radioembolization from 1/23/2020 to 10/21/2022. The diagnosis of HCC was made with multiphase, contrast-enhanced cross-sectional imaging of the liver, or biopsy using the Organ Procurement and Transplantation Network/United Network for Organ Sharing criteria [10].

Liver-Directed Therapy and Treatment Protocols

Y90 was performed as a two-phase process, including mapping angiogram and Y90 delivery. During mapping angiography, vascular evaluation of the celiac artery, superior mesenteric artery, proper hepatic artery, and all feeding hepatic arteries to the areas of tumor was performed. Contrast-enhanced cone-beam CT was also performed for all patients to confirm complete coverage of the tumor angiosome as well as calculate perfused volume for radioembolization. Medical Internal Radiation Dose (MIRD) was utilized and incorporated perfused volumes and lung shunt fraction from the mapping procedure. Radiation segmentectomy was performed with Y90 glass microsphere infusion (TheraSphere; Boston Scientific, Marlborough, MA, USA) via segmental or subsegmental delivery. During treatment, all feeding vessels to areas of the tumor were treated with target radiation doses greater than 200Gy to the perfused volume, and treatment was followed by imaging with Bremsstrahlung SPECT/CT in a single outpatient procedure. Following the results of LEGACY, target radiation doses were increased to greater than 400Gy to the perfused volume [1]. Patients were assessed for AEs via phone call at 24 hours as well as clinic appointment at 1 month. Laboratory AEs were assessed at target post-Y90 periods of 60 days and 180 days. Posttreatment imaging and laboratory values were obtained at 1 month.

Post-treatment dosimetry was evaluated using Mirada DBx Build 1.2.0 Simplicit^{90}Y dosimetry software. Pre-treatment diagnostic CT/MRI studies were incorporated with post-treatment SPECT nuclear medicine and CT

scans. Total liver and perfusion volumes, as well as tumor volumes, were defined; and post-treatment parameters tabulated using the multi-compartment dosimetry model.

Tumor mass (kg) was calculated using the following equation:

$$tumor\ volume(mL) \times 1.03(g/mL) \div 1000(g/kg)$$

Spheres delivered to tumor was calculated using the following equation:

$$\frac{tumor\ absorbed\ dose\left(\frac{J}{kg}\right) \times tumor\ mass(kg)}{50\left(\frac{J}{GBq}\right) \times sphere\ activity\ at\ delivery(Bq)} \times 10^9$$

Sphere concentration per tumor volume was calculated using the following equation:

$$spheres \div tumor\ volume(mL)$$

Sphere concentration per non-tumor volume was calculated using the following equation:

$$spheres \div (perfused\ volume - \ tumor\ volume)(mL)$$

SA at time of administration was recorded using the lot number of each infused vial, referenced from distribution. Weight and dose activity at time of calibration were documented. After referencing the delivered vials with the distributor, 4300Bq was used as the mean individual SA at time of calibration. Then, the standard decay pattern for yttrium-90 from calibration was used to determine the SA at time of delivery after referencing the corresponding day and hour of administration.

First cycle response to Y90 was recorded using the Modified Response Evaluation Criteria in Solid Tumors (mRECIST) in all patients with follow-up imaging < 120 days post-procedure and without any secondary treatment prior to imaging.

Primary Outcome

The cohort was followed longitudinally to a primary endpoint of HCC progression beyond transplant criteria. The primary assessment of outcome was performed using time to progression (TTP) defined as the time from first cycle Y90 until HCC progression. TTP analysis was censored for the following conditions: liver transplant (LT), election to pursue systemic therapy without tumor progression, lost to follow-up, all-cause mortality, or no evidence

of HCC progression at the time of last imaging. Censoring date was defined at the time of the disqualifying event with exception to no evidence of HCC progression at time of last imaging.

Pathology Results

The degree of targeted tumor necrosis was assessed in patients successfully bridged to LT. The percentage of tumor necrosis was estimated by a hepatobiliary pathologist and the percentage extracted from the synoptic liver transplant pathology report. The degree of necrosis was grouped as follows: no necrosis (0%), partial necrosis (< 50%), extensive necrosis (50 – 99%), complete necrosis (100%).

Post-Y90 Adverse Events

AEs post-Y90 were monitored within the 180-days following first cycle treatment. AEs were graded based on the common terminology criteria for adverse events (CTCAE) version 5.0 [11].

Statistical Methods

Data analysis was performed in JMP 13.0 (SAS Institute Inc.) with graphical output generated using Prism 8.0 (GraphPad Software Inc.). Linear regressions were analyzed in JMP and reported with the P-value and coefficient of determination (R^2). Univariate Cox regression analysis was used to determine variables associated with TTP. Univariate continuous values reaching $p < 0.050$ were dichotomized using logistic regression of the variable against HCC progression and using the receiver operating curve (ROC). Multivariate analysis of statistically significant univariate variables was also performed. Kaplan–Meier survival curves were generated in Prism and compared using log-rank tests. For logistic regression analysis, differences in the component variables and outcome were analyzed using Mann–Whitney, Fisher, and Chi-square tests.

RESULTS

Patient and Tumor Characteristics

57 patients with treatment-naive, solitary HCC with a median tumor size of 3.4cm (range, 1.2-6.8cm) were treated during the defined interval. All targeted tumors received a single treatment. Detailed treatment characteristics are listed in **Table 1**.

Table 1 Y90 Patient and Tumor Characteristics	
General Demographics	n = 57
Age at HCC Diagnosis (years), median (range)	66 (42 - 73)
Sex, self-reported, total male (%)	45 (79)
Child Pugh, total (%)	
A5	22 (39)
A6	15 (26)
B7	11 (19)
B8-B9	9 (16)
MELD Component and MELD, median (IQR)	
MELD-Na	9 (7 - 12)
ALBI Grade	
Grade 1	16 (28)
Grade 2	37 (65)
Grade 3	4 (7)
HCC Baseline	
Index HCC Diameter (cm), median (range)	3.4 (1.2 - 6.8)
Transplant Criteria at Diagnosis, total (%)	
Milan	51 (89)
UNOS-DS	6 (11)
AFP (ng/mL), median (IQR)	6.1 (3.6 - 44)
Treatment Response	
Initial Treatment Follow-up (days), median (IQR)	92 (42 - 110)
Targeted mRECIST, total (%) | % of available	
Complete Response	41 (72) | (79)
Partial Response	9 (16) | (17)
Stable Disease	1 (2) | (2)
Disease Progression	1 (2) | (2)
Unable to Assess	5 (9)
Overall mRECIST, % (total)| % of available	
Complete Response	38 (67) | (73)
Partial Response	8 (14) | (15)

Stable Disease	2 (4) | (4)
Disease Progression	4 (7) | (8)
Unable to Assess	5 (9)
Bridge to Transplant Outcomes	
Status, total (%)	
Liver Transplant	14 (25)
Active	27 (47)
Tumor Progression	4 (7)
Censored	12 (21)
Follow-Up and Time to Outcome	
Liver Transplant (months), median (IQR)	7 (5 - 8)
Active (months), median (IQR)	12 (8 - 24)
Tumor Progression (months), median (IQR)	6 (3 - 9)
Censored (months), median (IQR)	4 (2 - 8)
Transplant Pathology	**n = 14**
Target Tumor Necrosis (%), median (range)	99 (80 - 100)
Degree of Necrosis, total (%)	
Extensive	9 (64)
Complete	5 (36)
Abbreviations: ^{90}Yittrium (^{90}Y), hepatocellular carcinoma (HCC), interquartile range (IQR), model of end-stage liver disease (MELD), alpha fetoprotein (AFP), modified response evaluation criteria in solid tumors (mRECIST).	

Using tumor absorbed dose and non-tumor absorbed dose from Voxel-based dosimetry, the median sphere concentration within tumor was 12,339 microspheres/mL, and the median sphere concentration into nontumoral liver was 7,912 microspheres/mL. Sphere concentration within tumor exhibited a weak, inverse correlation with perfused volume, as lower perfused volumes were associated with higher spheres concentrated into tumor (R^2=0.25; **Figure 1a**). Similarly, sphere concentration into nontumoral liver inversely correlated with perfused volume, as larger perfused volumes were associated with a higher rate of microspheres/mL tissue (R^2=0.39, **Figure 1a**). Sphere concentration into tumor and sphere concentration into non-tumor liver demonstrated a direct, linear correlation (R^2=0.72, **Figure 1b**).

Sphere concentration into tumor was less than 20,000 microspheres/mL in 83% of tumors (n=47). As tumor diameter increased, the total spheres delivered to tumor demonstrated a positive, non-linear relationship (R^2=0.33, p<0.001, **Figure 2**).

Mass balance was analyzed to compare the total sphere count in each vial prior to delivery with the total sphere count into tumor and non-tumor perfused tissue, which demonstrated median sphere recovery rate of 97% (range,

95-99%).

Imaging and Pathologic Outcomes

Initial target lesion complete response was observed in 41 (79%) of 52 patients and partial response was observed in 9 (17%) of 52 patients for an objective response rate of 96% (**Table 1**). Duration of response was evaluated in the 50 patients with an objective response. 98% of treated tumors demonstrated a durable response at 2 years. A 2-year progression rate of 11% was observed, demonstrating that median time to progression was not reached (**Figure 3**). Dose to volume, tumor sphere concentration, and perfused sphere concentration were statistically significant variables associated with time to progression by Cox proportional-hazard univariate analysis. Yet, multivariate analysis revealed dose to perfused volume as the only significant variable associated with time to progression (**Table 2**).

Table 2 ^{90}Y Therasphere Dosimetry and Time to Progression Analysis			
Dosimetry		Cox Proportional Hazards Analysis of Time to Progression	
Pre-Treatment Dosimetry		Univariate p-Value	Multivariate p-Value
Target Volume (mL), median (range)	140 (25 - 488)	0.303	
Target Dose to Volume (Gy), median (range)	474 (177 - 1290)	0.006	0.033
Target Dose to Volume ≥ 400 Gy, total (%)	45 (79)		
Vial Size (GBq), median (range)	4.5 (1.6 - 13)	0.160	
Dose Activity at Delivery (GBq), median (range)	1.6 (0.3 - 4.5)	0.881	
Activity per Sphere (Bq), median (range)	1428 (412 - 2589)	0.143	
Lung Shunt Fraction (%), median (range)	6.6 (0.7 - 27)	0.627	
Post-Treatment Dosimetry			
Total Liver Volume (mL), median (range)	1650 (904 - 3427)	0.424	
Tumor Volume (mL), median (range)	16.6 (0.80 - 205)	0.594	
Perfusion Volume (mL), median (range)	113 (33.6 - 442)	0.670	
Non-Tumor Volume (mL), median (range)	91.3 (16.3 - 357)	0.480	
Tumor to Perfused Mass Ratio, median (range)	0.14 (0.01 - 0.58)	0.720	
Perfused Liver Mass Fraction (%), median (range)	6.0 (2.3 - 21)	0.627	
Perfused Non-Tumor Tissue Mass Fraction (%), median (range)	5.1 (1.0 - 19)	0.744	
Tumor Absorbed Dose (Gy), median (range)	692 (252 - 1776)	0.550	
Tumor Sphere Concentration (spheres/mL), median (range)	12,339 (2,689 - 37,649)	0.035	0.411
Perfused Volume Sphere Concentration (spheres/mL), median (range)	9,199 (2,787 - 24,225)	0.074	0.773
Perfused Non-Tumor Dose (Gy), median (range)	521 (256 - 1322)	0.902	
Non-Tumor Sphere Concentration (spheres/mL), median (range)	8,688 (3,532 - 23,702)	0.069	0.762
Tumor / Non-Tumor Dose Ratio, median (range)	1.3 (0.5 - 2.7)	0.178	

Abbreviations: ^{90}Yittrium (^{90}Y), interquartile range (IQR), Gray (Gy), giga-becquerel (GBq), becquerel (Bq).

Adverse Events

Patients were followed up to 6 months for treatment-related AEs associated with radiation segmentectomy. No procedure-related AEs were noted. At 60 days, treatment related AEs were noted in 19 patients (37%) with no patients experiencing grade 3 or higher adverse events. At a median follow-up of 179 days, only 2 grade 3 AEs were noted, platelet count decrease (**Table 3**). AEs were not associated with nontumoral absorbed dose (p=0.47).

Table 3 ^{90}Y Therasphere 60-Day and 180-Day AE Outcomes	
60-Day Adverse Events	
AE Follow-up (days), median (IQR)	63 (37 - 84)
Adverse Events, total (%)	
All Grade AE	19 (37)
No AE	33 (63)
Unable to Assess n = 5	
Any Grade 3 AE, total (%)	
Any Grade ≥ 3	0 (0)
No AE or Grade ≤ 2	52 (100)
Unable to Assess n = 5	
Albumin AEs, total (%)	
None	40 (77)
Grade 1	5 (10)
Grade 2	7 (13)
Unable to Assess n = 5	
Bilirubin AEs, total (%)	
None	42 (81)
Grade 1	10 (19)
Unable to Assess n = 5	
Platelet AEs, total (%)	
None	44 (96)
Grade 1	1 (2)
Grade 2	1 (2)
Unable to Assess n = 11	
180-Day Adverse Events	
AE Follow-up (days), median (IQR)	179 (162 - 196)
Adverse Events, total (%)	
All Grade AE	20 (53)
No AE	18 (47)
Unable to Assess n = 19	
Any Grade 3 AE, total (%)	

Any Grade ≥ 3	2 (5)
No AE or Grade ≤ 2	36 (95)
Unable to Assess n = 19	
Albumin AEs, total (%)	
None	30 (79)
Grade 1	5 (13)
Grade 2	3 (8)
Unable to Assess n = 19	
Bilirubin AEs, total (%)	
None	28 (74)
Grade 1	8 (21)
Grade 2	2 (5)
Unable to Assess n = 19	
Platelet AEs, total (%)	
None	27 (71)
Grade 1	6 (16)
Grade 2	3 (8)
Grade 3	2 (5)
Unable to Assess n = 19	
Abbreviations: ^{90}Yittrium (^{90}Y), interquartile range (IQR), Gray (Gy), adverse event (AE), eastern cooperative oncology group (ECOG), model of end-stage liver disease (MELD).	

DISCUSSION

The patient outcomes within this cohort add to the growing literature supporting radiation segmentectomy with glass microspheres for the treatment of early-stage HCC in patients with solitary tumors. The localized objective response rate of 96% aligns with other reported outcomes in literature [1, 12, 13]. Comparably, durable treatment response greater than 2 years was achieved in 98% of treated lesions, and only 11% of patients demonstrated progression at 2 years.

The importance of individual SA is becoming more integral piece of personalized dosimetry [13, 14]. SA ≥ 327Bq and ≥ 446Gy are more likely to generate CPN in patients who have received ablative radiation segmentectomy [13]. In this cohort, SA did not demonstrate a statistically significant difference in TTP, as SA for every case was above the cutoff threshold identified previously for optimal outcomes [13]. On the other hand, early arterial stasis can be seen during the use of resin microspheres, related to its lower SA and need for larger volumes of microspheres to reach the intended dose to target, which may result in early termination of Y90 delivery and failure to completely deliver the prescribed dose [15]. This could imply that limited space exists within the tumor microenvironment for

efficient microsphere delivery. Similarly, the results of this study highlight the importance of SA on imaging and pathologic treatment response, as it relates to limited space within the tumor to concentrate microspheres and deliver an ablative dose. In this study, the desired dose was delivered in *all* cases, which is similar to other publications involving the use of glass microspheres [1, 3, 5, 12, 13]. Based on **Fig. 1**, as perfused volumes decrease, tumor sphere concentration increases. While this study was not designed to evaluate the *maximum* sphere concentration allowed in tumor, tumor sphere concentrations rarely increased greater than 20,000 microspheres/mL, even at perfused volumes under 100mL, when spheres are most concentrated in the tumor. This, and studies with resin Y90 microsphere delivery ending in stasis, may suggest that sphere concentration into tumor becomes *inefficient* above a saturation point.

If 20,000 microspheres/mL were used as the cutoff for efficient microsphere saturation within the tumor microenvironment, the minimum threshold for SA could be calculated to achieve a target dose of 400Gy to the perfused volume. Using MIRD dosimetry, the minimum SA would need to be 412Bq/sphere to achieve a target dose of 400Gy in tumors within the size range of this study, 1.2–6.8 cm. This is equivalent to planning treatment within 8.5 days after initial calibration of glass microspheres.

While a recent study has demonstrated dose thresholds when treating larger liver volumes with resin microspheres, no dose threshold was noted for segmental deliveries despite higher radiation doses to non-tumoral liver, suggesting that AEs are more associated with treatment volume rather than dose [9]. Notably, resin microspheres are much more likely to reach stasis and result in homogeneous saturation of the perfused non-tumoral liver, resulting in a greater amount of hepatic lobules at risk [8, 15]. However, *ablative* radiation segmentectomy with glass microspheres is well-tolerated with limited AEs in patients with preserved liver function [16]. Similarly, AE rates were very low in this cohort, despite ablative doses to normal tissue. This likely reflects the impact of total liver volume treated and limited non-tumoral liver perfusion as well as smaller spherical concentration and heterogeneous distribution to normal tissue with glass microspheres, resulting in fewer hepatic lobules at risk.

Several limitations in this study exist, including its retrospective design and relatively small sample size. Another potential limitation of this study is the use of SPECT/CT in post- Bremsstrahlung Y90 imaging. SPECT/CT and PET/CT have demonstrated good agreement in regions of treatment on prior studies. However, PET/CT had been shown to overestimate activity in regions of low or no activity [17]. Therefore, any estimates of uptake in areas of low absorbed dose would be at risk for *relative* underestimation of dose. Additionally, mass balance of total spheres per vial, distributed into to tumor and non-tumor liver, was appropriately accounted for in this cohort. Finally, 4300Bq was used as the mean activity per sphere and some variability may exist between each dose. However, this activity was directly correlated with individual lot numbers from the distributor, and variations between each vial should be relatively small. This number also closely corresponds to a recent study evaluating Bq/sphere with glass microspheres [8].

In conclusion, SA plays a critical role in radiation segmentectomy, as limited space exists within the tumor bed for efficient sphere concentration. *Higher* individual SA allows reproducible delivery of ablative target radiation doses to tumor with spheres that will undergo more decays per sphere and increase radiation damage to the targeted tumor. Increasing sphere concentration beyond its saturation point results in a higher concentration of microspheres to non-tumoral liver and greater likelihood of adverse events. Therefore, if sphere concentration to tumor begins to become inefficient at 20,000 microspheres/mL, SA should be 412Bq/sphere, or 8.5 days from initial calibration, to achieve a minimum target dose of 400Gy.

ABBREVIATIONS

Y90	Yttrium-90
BCLC	Barcelona Clinic Liver Cancer
HCC	Hepatocellular carcinoma
CPN	Complete Pathologic Necrosis
SA	Sphere activity
AE	Adverse event
MIRD	Medical internal radiation dose
mRECIST	Modified Response Evaluation Criteria in Solid Tumors

STATEMENTS AND DECLARATIONS

Acknowledgements

The authors would like to thank Katie Routh and Tim Griffith for their assistance with this project.

Ethics Approval and Consent to Participate

The study was designed as a retrospective analysis and approved by the Ochsner Clinic Foundation Institutional Review Board (protocol 2019.308, principal investigator Tyler Sandow) and in accordance with the ethical guidelines set forth by the Declaration of Helsinki.

Consent for Publication

Not applicable.

Availability of data and material

The datasets used and/or analyzed during the current study are available from the corresponding author on reasonable request.

Competing Interests

T.S. is an advisor and consultant for Boston Scientific. J.G. is an advisor and consultant for Boston Scientific. A.C. is a consultant for Boston Scientific. P.T. receives grant funding from Boston Scientific. The authors reported no other potential conflicts of interest for this work.

Funding

Not applicable.

Author Contribution

All authors contributed to the study conception and design. Material preparation, data collection, and analysis were performed by Tyler Sandow, Juan Gimenez, Kelley Nunez, and Paul Thevenot. All authors contributed to data gathering and manuscript editing. All authors, read, edited, and approved the final manuscript.

References

1. Salem R, et al. Yttrium-90 Radioembolization for the Treatment of Solitary, Unresectable HCC: The LEGACY Study. Hepatology. 2021;74(5):2342–52.
2. Reig M, et al. BCLC strategy for prognosis prediction and treatment recommendation: The 2022 update. J Hepatol. 2022;76(3):681–93.
3. Vouche M, et al. Unresectable solitary hepatocellular carcinoma not amenable to radiofrequency ablation: multicenter radiology-pathology correlation and survival of radiation segmentectomy. Hepatology. 2014;60(1):192–201.
4. Gabr A, et al. Correlation of Y90-absorbed radiation dose to pathological necrosis in hepatocellular carcinoma: confirmatory multicenter analysis in 45 explants. Eur J Nucl Med Mol Imaging. 2021;48(2):580–3.
5. Toskich B, et al. Pathologic Response of Hepatocellular Carcinoma Treated with Yttrium-90 Glass Microsphere Radiation Segmentectomy Prior to Liver Transplantation: A Validation Study. J Vasc Interv Radiol. 2021;32(4):518–526e1.
6. Gabr A, et al. Liver Transplantation Following Yttrium-90 Radioembolization: 15-Year Experience in 207-Patient Cohort. Hepatology. 2021;73(3):998–1010.
7. Toskich BB, Liu DM. Y90 Radioembolization Dosimetry: Concepts for the Interventional Radiologist. Tech Vasc Interv Radiol. 2019;22(2):100–11.
8. Pasciak AS, et al. The number of microspheres in Y90 radioembolization directly affects normal tissue radiation exposure. Eur J Nucl Med Mol Imaging. 2020;47(4):816–27.
9. Kokabi N et al. *Voxel-based dosimetry predicting treatment response and related toxicity in HCC patients treated with resin-based Y90 radioembolization: a prospective, single-arm study*.Eur J Nucl Med Mol Imaging, 2023.
10. Wald C, et al. New OPTN/UNOS policy for liver transplant allocation: standardization of liver imaging, diagnosis, classification, and reporting of hepatocellular carcinoma. Radiology. 2013;266(2):376–82.
11. *Common Terminology Criteria for Adverse Events (CTCAE).v.5.0*. [cited 2023; Available from: https://ctep.cancer.gov/protocoldevelopment/electronic_applications/docs/ctcae_v5_quick_reference_5x7.pdf.
12. Kim E, et al. Radiation segmentectomy for curative intent of unresectable very early to early stage hepatocellular carcinoma (RASER): a single-centre, single-arm study. Lancet Gastroenterol Hepatol. 2022;7(9):843–50.
13. Montazeri SA, et al. Hepatocellular carcinoma radiation segmentectomy treatment intensification prior to liver transplantation increases rates of complete pathologic necrosis: an explant analysis of 75 tumors. Eur J Nucl Med Mol Imaging. 2022;49(11):3892–7.
14. Salem R, et al. Clinical, dosimetric, and reporting considerations for Y-90 glass microspheres in hepatocellular carcinoma: updated 2022 recommendations from an international multidisciplinary working group. Eur J Nucl Med Mol Imaging. 2023;50(2):328–43.
15. Piana PM, et al. Early arterial stasis during resin-based yttrium-90 radioembolization: incidence and preliminary outcomes. HPB (Oxford). 2014;16(4):336–41.

16. De la Garza-Ramos C, et al. Biochemical Safety of Ablative Yttrium-90 Radioembolization for Hepatocellular Carcinoma as a Function of Percent Liver Treated. J Hepatocell Carcinoma. 2021;8:861–70.
17. Yue J, et al. Comparison of quantitative Y-90 SPECT and non-time-of-flight PET imaging in post-therapy radioembolization of liver cancer. Med Phys. 2016;43(10):5779.

Figures

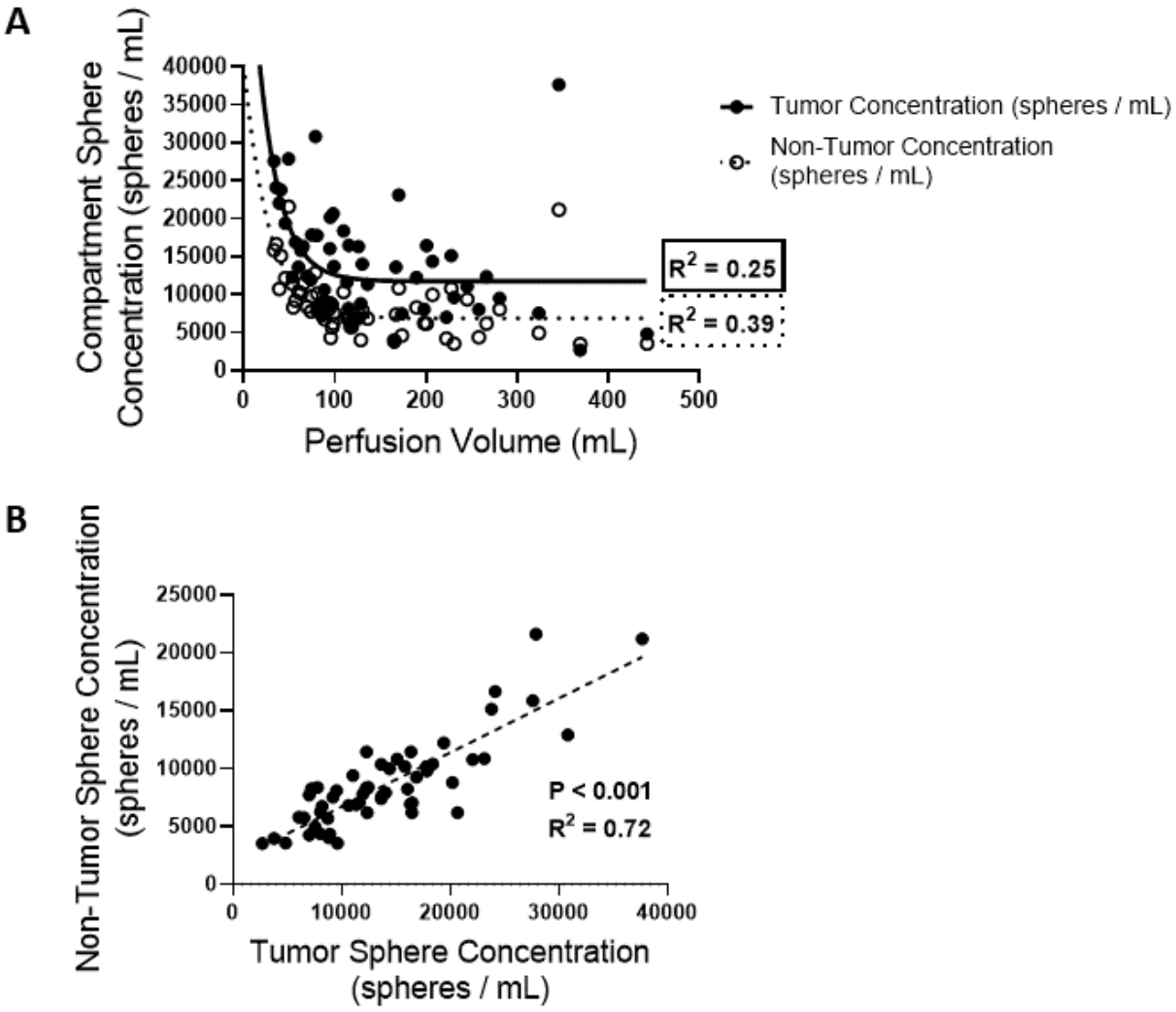

Figure 1

Sphere Concentration relationship to perfused volume (**A**) and Tumor Sphere Concentration relationship to Non-Tumor Sphere Concentration (**B**)

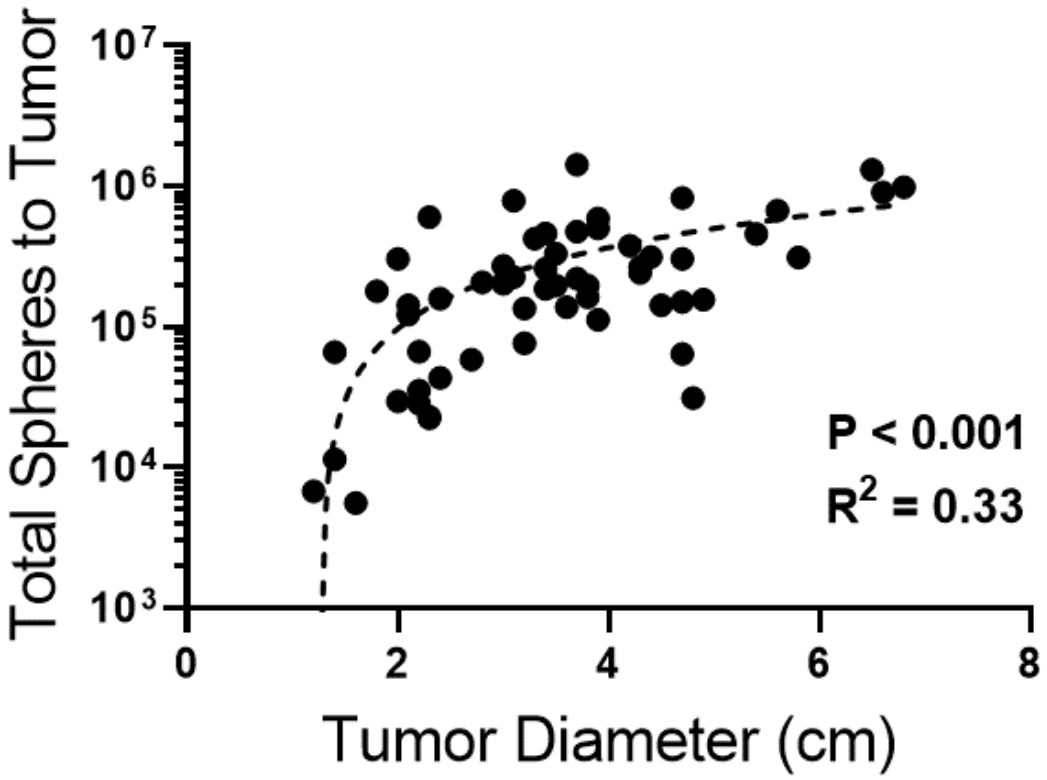

Figure 2

Total Microspheres Delivered to Tumor based on Tumor Diameter

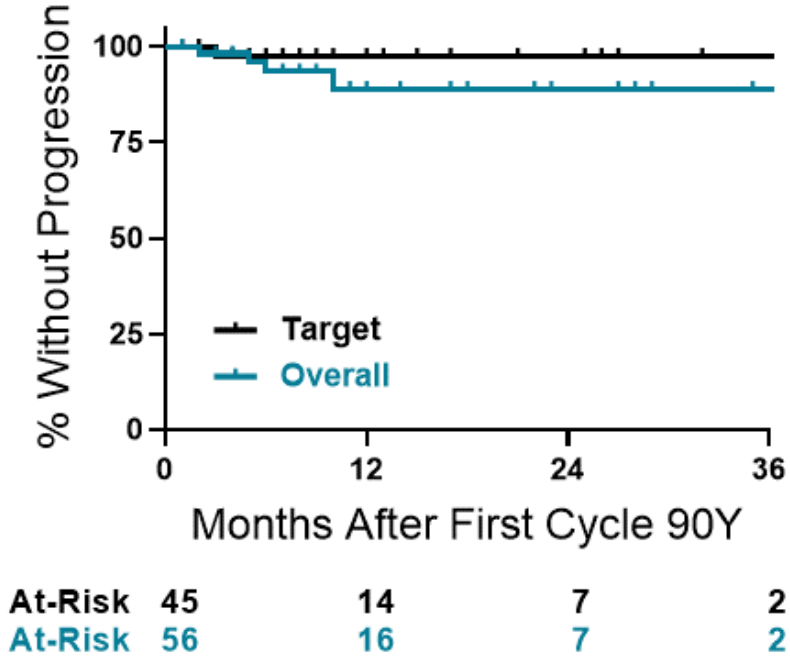

Figure 3

Kaplan-Meier analysis of Time to Progression for Target Tumor and Overall Response